TEST OF THE SECOND MODEL OF THE GCFR STEAM GENERATOR CAVITY CLOSURE PLUG

J. P. CALLAHAN, G. C. ROBINSON, W. G. DODGE
Oak Ridge National Laboratory,
P.O. Box Y, Oak Ridge, Tennessee 37830, U.S.A.

ABSTRACT

As part of its participation in the program to develop a 300 MW(e) gas-cooled fast reactor (GCFR) demonstration power plant, the Oak Ridge National Laboratory (ORNL) is conducting a series of structural model tests. One of the tasks of the ORNL effort provides for the design, analysis and/or testing of small-scale models of the PCRV penetration closure plugs. The principal objectives are to determine structural response of the plugs to normal operating pressures and to substantial overpressurization. The tests also provide reliable data for verification of analysis methods. Included in the testing program are models of both the steam generator cavity closure and central core cavity closure plugs.

Thus far, two models of the steam generator cavity closure series have been tested. The first model which represented the original GA design was pressurized to 75.8 MPa (11,000 psi) without sustaining cracking of the concrete or failure of the plug although yielding of the metallic components was recorded by attached strain gages. The results of the first test were described in the SMiRT-4 paper H6/6.

The second steam generator cavity closure plug model represents a modification of the original design to reduce excessive conservatism. The thickness of the plug was reduced to one-half the original plug, and the steel reinforcement was significantly reduced.

Following 10 pressurization cycles from no load to the maximum cavity pressure (MCP) of 10.08 MPa (1462 psig), the model was pressurized in steps until failure occurred. No visual indications of distress were evident prior to failure, although the strains on metal components exceeded 1.2% and strains recorded by the embedded concrete gages were of the order of 1%. Failure occurred by abrupt punching shear at approximately 99.3 MPa (14,000 psig), thereby expelling the central section with considerable force. The failure surface was that of a truncated cone.

Comparisons of strains and deformations calculated using the finite-element code ADINA with experimental values indicated fair agreement. The differences between calculated and measured values are attributed to difficulties in representing the boundary conditions analytically, and to the employment in ADINA of inadequate constitutive equations to represent the nonlinear response of concrete under complex states of stress.

The results of this test demonstrated the inherent strength of the closure plug and also showed that calculations made using a finite-element code in conjunction with state-of-the-art concrete constitutive equations provide conservative predictions of the failure process.

---

*Research sponsored by the Division of Reactor Research and Technology, U.S. Department of Energy under contract W-7405-eng-26 with the Union Carbide Corporation.

1. INTRODUCTION

The Oak Ridge National Laboratory (ORNL) under sponsorship of the U.S. Department of Energy is conducting design verification and support studies of the prestressed concrete reactor vessel (PCRV) for the 300-MW(e) GCFR demonstration power plant. These studies are planned and conducted in close cooperation with the General Atomic Company (GA) which has the overall design and development responsibility. One of the ORNL studies consists of the design, analysis, and testing of small-scale models of the PCRV closure plugs. The primary objective is to determine structural response of the plugs both to normal operating pressure and to substantial overpressurization. These tests also provide reliable data for verification of analysis methods. Included in the program are tests of models of both the steam generator cavity and reactor core cavity closures.

Thus far, two 1/15-scale models of the steam generator cavity closure have been tested. The first model [1], which represented the original design, was subjected to a pressure in excess of 7.5 times the design value without experiencing detectable cracking of the concrete or failure of the plug although yielding of the metallic components was recorded by attached strain gages. A second steam generator cavity closure model was based on a redesign to reduce the excessive conservatism of the first model. The thickness of the plug and the steel reinforcement were reduced significantly. This paper describes the test of the second steam generator cavity closure model and related analytical studies.

2. PROTOTYPE DESCRIPTION

The 300-MW(e) GCFR demonstration plant utilizes a multicavity PCRV having large-diameter closures for both the reactor cavity and steam generator cavities. The design maximum cavity pressure is 10.08 MPa. The prototype steam generator cavity closure plug shown in Fig. 1 represents the reference design used for the models. In these models the concrete is confined on the inner and bottom surfaces by a relatively thin steel liner; ring forgings are attached to the top of both inner and outer wall liners. The function of the rather large forging attached to the outer liner is to transfer the resulting pressure loads from the plug to the adjacent axial prestressing tendons of the PCRV. This transfer is accomplished by means of a series of circumferentially spaced two-force members called toggles. The toggles are inclined at an angle of 25 deg from the vertical and induce a radial compression loading to the ring forging; thus, together with the lateral pressure of the coolant, they produce a circumferential prestress on the plug which remains directly proportional to the pressure loading induced by the reactor coolant. The helium circulator is supported by a heavy-walled cylindrical steel component attached to the bottom of the plug's inner liner. The reader is referred to Ref. [1] for a more detailed description of the original prototype plug design.

3. MODEL DESCRIPTION

Figure 2 shows a cross section of the second steam generator cavity model of the test series. The model represents a linear scaling of all physical features of the prototype except that the depth of the plug has been reduced by one-half and the shear console reinforcement (described in Ref. 1) has been eliminated.

The steel materials specified for the prototype plugs, consisting of ASTM A508 class 1 forgings, ASTM A537 class 1 plate, and ASTM A615 grade 60 reinforcing bars, are relatively common low-alloy steels but are not available in small lots. Therefore, we elected to utilize available low-carbon steels and to apply various heat treatments, as required, to effect simulation of the proper stress-strian curves. It was assumed that the stress-strain curves of the model and prototype steel components could be considered reasonably matched if correspondence were maintained up to about 1% strain.

A microconcrete mixture was designed to simulate ultimate strength and modulus of elasticity of the prototype concrete. The microconcrete utilized a crushed limestone aggregate that was screened to pass a No. 8 standard sieve and be retained on a No. 50 sieve; the modulus of elasticity was 32.25 GPa and compressive strength was 59.39 MPa. The internal network of modeled conventional steel reinforcing bars represented by the heavy lines in Fig. 2 was included in the concrete section of the plug. Bright basic AISI 1010 wire having 2.45 and 1.27 mm diameters was used to represent the No. 10 and No. 6 rebar respectively. The wire was deformed using the University of Illinois knurling machine and then was heat treated by annealing to obtain the yield strength specified for ASTM A615 rebar. Since the model was expected to fail prior to any appreciable work hardening, the matching of yield strengths rather than ultimate strengths was the primary criterion used in simulating mechanical properties of the prototype metallic components.

Figure 3 shows a cross section of the model positioned for testing in the steel test fixture. The test fixture was designed to permit pressure testing to 138 MPa. A threaded bushing assembly was used to secure the model in the vessel as shown in Fig. 3, and sealing was accomplished by elastomeric O-ring seals. The restraining system used for the model differed significantly from that of the prototype; a ball-bearing support (Fig. 3) was selected to provide sufficient strength to preclude premature failure during the overpressurization phase of the test. However, this system did not necessarily produce the same radial component of load on the outer ring forging as the toggle system. In particular, the pressure acting along the outer wall of the plug tends to deflect the forging inwardly, while the ball bearing support places a restraint on this deformation that would not exist with the toggle support of the prototype. Thus, less radial compression was probably produced on the model forging than would be produced using the prototype toggle system. Detailed analysis has shown that, because of the massiveness of the forging, this effect was rather small and did not significantly affect the results of this test. Penetrations were provided in the bottom of the vessel to permit pressurization and to provide access for up to 24 channels of instrumentation. The beam gage plug assembly at the bottom of the vessel cavity (Fig. 3) served as a mounting block for six beam gages to monitor vertical movement of the bottom face of the plug and also served as a ballast to reduce the total potential energy of the hydraulic fluid contained within the vessel. The top of the model was instrumented using 10 commercial displacement transducers, three of which monitored vertical displacement and seven monitored radial displacements.

Strain instrumentation consisted of 23 electrical resistance strain gages bonded to metallic components, and two, three-gage rosettes embedded in the microconcrete as the same vertical position and orientation, but spaced 90 deg apart. These embedment gages were of a special miniaturized type consisting of electrical resistance strain gages that were bonded to thin epoxy strips and subsequently encapsulated in epoxy. A view of the model with all strain measuring instrumentation attached is shown in Fig. 4.

4. MODEL TEST

The model was subjected to ten pressurization cycles to 10.08 MPa. After each cycle, the pressure was reduced to 2.76 MPa; the pressure and response data were recorded for all cycles. During the eleventh cycle, the model was pressurized in steps until the ultimate capacity of the plug was achieved. Failure occurred by punching shear at 99.3 MPa, which was approximately ten times the design pressure of the prototype. Although a surface strain of 1.2% was measured at failure, no concrete cracking was evident prior to failure as viewed by the video monitor. Immediately prior to failure one vertically oriented embedment strain gage indicated almost complete recovery of strain prior to failure, possibly indicating that the failure surface developed and coincided with this gage. Figure 5 shows the inner and outer sections formed at failure.

5. MODEL ANALYSIS

A pretest analysis was conducted to provide an estimate of the strength and potential mode of failure of the model. The finite element code ADINA [2] which employs material constitutive models to represent the nonlinear stress-strain response of the steel and concrete materials, was used to perform this analysis; the element layout is shown in Fig. 6. Axisymmetric solid elements were used to represent all aspects of the geometry with the exception of the embedded reinforcement, which was represented by two-force truss members. The solid element boundaries were made to coincide with the location of the reinforcing members lying in vertical planes and the node positions to coincide with the location of the circumferential reinforcement. The resulting analytical representation of the model employed 171 nodes, 53 elastic-plastic steel elements, 54 concrete elements and 30 truss elements.

A bilinear kinematic hardening material model was used to represent the stress-strain response of the elastic-plastic steel elements (shown shaded in Fig. 6). A yield point of 220.6 MPa was used for the inner and outer ring forging; 482.6 MPa was used for the inner wall liner and 517.1 was used for the remaining steel components. An initial elastic modulus of 206,800 MPa, a Poisson ratio of 0.28, and a hardening modulus of 6895 MPa was used for all steel components. The constitutive model used to represent the concrete response was the same as described previously in Ref. [1].

In the analysis the model was subjected to a monotonic load by increasing pressure in 3.45-MPa increments to a final value of 68.9 MPa. The first indication of distress occurred at 27.5 MPa when a minor concrete tensile crack appeared in an element near the outer ring forging. This cracking spread across the adjacent elements as the pressure increased. At a pressure of 37.9 MPa, plastic yielding began at the intersection of the upper ring forging and the outer wall, and slowly spread inwardly and upwardly as the pressure increased. By the time the pressure reached 55.2 MPa, approximately half of the outer ring forging had experienced plastic yielding, and significant yielding had occurred in the circulator support and in the inner wall liner at its intersection with the circulator support.

At a pressure of 51.7 MPa, the analysis indicated crushing beginning in the concrete adjacent to the outer ring forging. When this occurred, the material stiffnesses for these elements were set to zero, which meant that they no longer provided restraint for the outer ring forging. At 62 MPa, the analysis indicated that the concrete adjacent to the outer ring forging had been crushed, and adjacent elements below this area in alignment with the toggle action were cracked.

At the maximum pressure of 68.9 MPa, the analysis showed the outer ring forging, the upper portion of the outer wall liner, the upper portion of the circulator support, the bottom liner, and the bottom portion of the inner wall liner had undergone plastic deformation. The concrete between the outer ring forging and the circulator support bottom liner intersection was either cracked or crushed. Thus, at this pressure, the plug was expected to be approaching its ultimate pressure capacity.

6. COMPARISON OF ANALYTICAL AND EXPERIMENTAL RESULTS

Displacements were measured by the 16 separate transducers described previously. In general, each transducer had a corresponding one which differed only in angular position. In order to provide a basis for comparison of vertical displacements, the calculated values were adjusted using a constant factor to account for the vertical rigid body motion of the model due to seating of the hold-down assembly. This constant was chosen so as to force agreement between calculated and measured vertical displacements of the upper ring forging. No such adjustment was necessary for the comparison of radial displacements. Calculated and experimental vertical displacements of the bottom liner at a radial position of 9.87 cm are shown in Fig. 7. In general, good agreement was seen between calculated and experimental vertical displacements as shown in this figure up to the 68.9 MPa maximum pressure predicted by ADINA; however, the analysis indicated greater stiffness for the model than was demonstrated by the experimental values. Rather poor agreement was seen between the calculated and experimental radial displacements. The two primary reasons for the lack of agreement were inconsistency in modeling the effect of the hold-down system and improper modeling of the post failure condition in the concrete material constitutive model.

An example of strains recorded by electrical resistance strain gages bonded to the outer liner is shown in Fig. 8. The experimental values of the circumferential strains on both the inside and outside surfaces of the liners are larger than those predicted by ADINA. These results are consistent with the fact that for triaxial states of stress the concrete material constitutive model used in ADINA is inherently too stiff. This same effect was seen for the axial strains where the experimental values were generally greater than the calculated values until concrete crushing is predicted. When crushing occurs, the axial thrust normally transmitted by the concrete is transferred to the liner and causes the abrupt change in slope of the analytical results as seen in Fig. 9.

The experimental strains measured by the concrete embedment strain gages were consistently larger than the calculated values as shown in Fig. 10. This trend tends to reinforce the hypothesis that the concrete constitutive model used in ADINA was too stiff for the triaxial stress conditions that were measured during the test.

7. CONCLUSIONS

This test demonstrated a significant overload capacity of the half-thickness version of the PCRV steam generator cavity closure plug design. The pressure at failure which was 99.3 MPa was nearly ten times the design pressure of 10.08 MPa. Comparisons of experimental and analytical results indicate that improved constitutive equations for concrete are needed to provide more accurate and less conservative estimates of the pressure response of this type of structure. Although failure occurred by punching shear, both the steel and concrete exhibited high inelastic strains.

REFERENCES

1. DODGE, W. G., ROBINSON, G. C., AND CALLAHAN, J. P., "Development of the PCRV Steam Generator Cavity Closure for the GCFR," *Nuclear Engineering and Design* 45, 523-31 (1978).
2. BATHE, K. J., *ADINA, A Finite Element Program for Automatic Dynamic Incremental Analysis,* Massachusetts Institute of Technology Report 82448-1 (September 1975, revised May 1976).

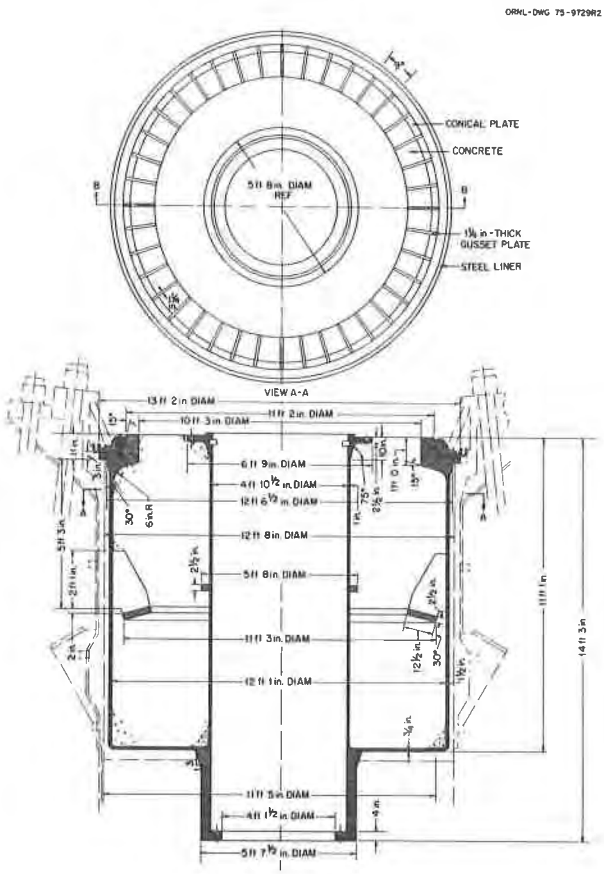

Fig. 1. Plan and vertical sections of the prototype steam generator cavity closure plug selected for the first 1/15-scale model test.

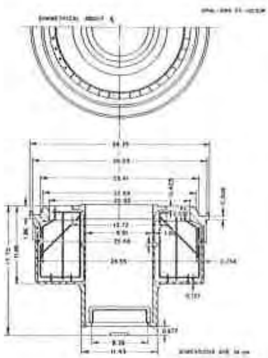

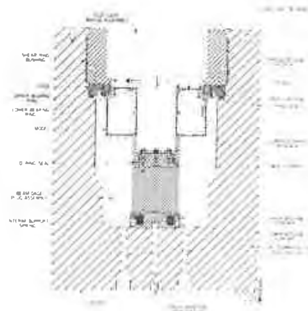

Fig. 2. Plan and vertical section of the 1/15-scale model of the 300-MW(e) GCFR PCRV steam generator cavity closure plug.

Fig. 3. Cross section of the 1/15-scale half-thickness steam generator cavity closure plug model positioned for testing in the test fixture.

Fig. 4. View of instrumented half-thickness model.

Fig. 5. Posttest view of inner and outer failed sections of the half-thickness model.

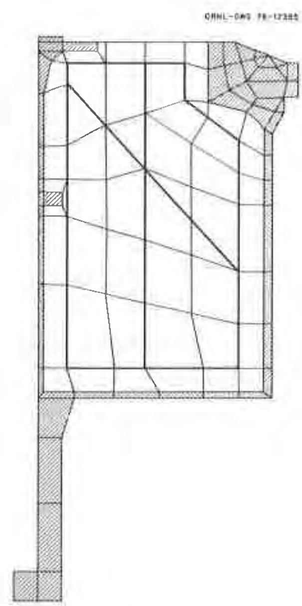

Fig. 6. Mesh used for the finite-element analysis of the 1/15-scale half-thickness steam generator cavity closure model.

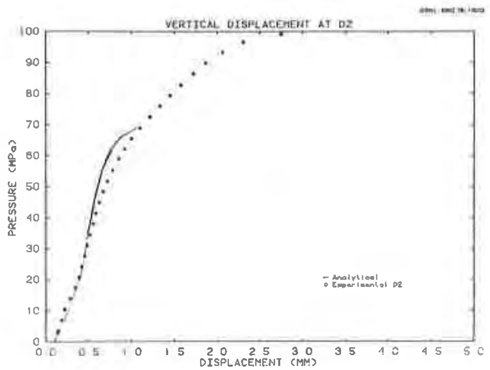

Fig. 7. Vertical displacement of the bottom liner at a radial position of 9.78 cm.

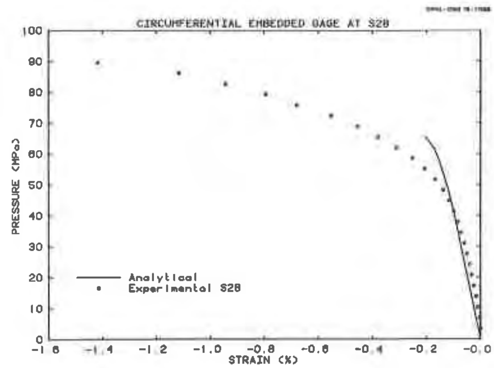

Fig. 8. Circumferential strain on the outside surface of the upper portion of the outer liner.

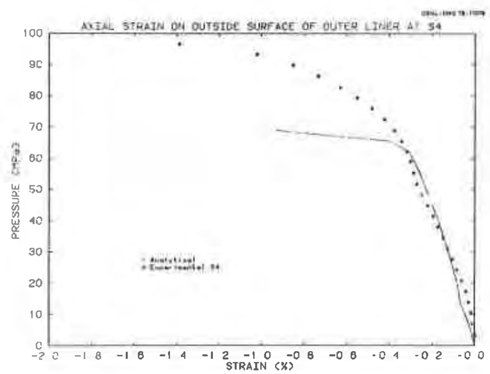

Fig. 9. Axial strain on the outside surface of the upper portion of the outer liner.

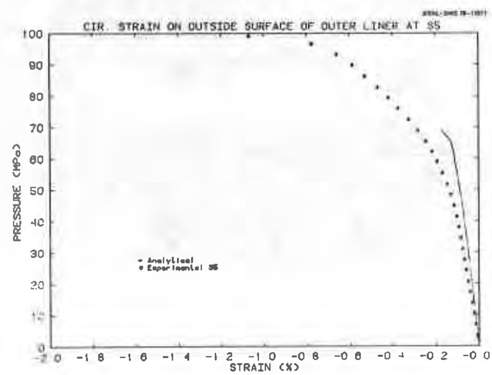

Fig. 10. Circumferential strain at gage embedded in concrete.